The Astrophysical Journal, 626:1102–1109, 2005 June 20

DETERMINATION OF LOW-ENERGY CUTOFFS AND TOTAL ENERGY OF NONTHERMAL ELECTRONS IN A SOLAR FLARE ON 2002 APRIL 15

Linhui Sui,[1] Gordon D. Holman, and Brian R. Dennis
Laboratory for Astronomy and Solar Physics, Code 612.1, NASA Goddard Space Flight Center, Greenbelt, MD 20771
Received 2005 January 14; accepted 2005 March 5

ABSTRACT

The determination of the low-energy cutoff to the spectrum of accelerated electrons is decisive for the estimation of the total nonthermal energy in solar flares. Because thermal bremsstrahlung dominates the low-energy part of flare X-ray spectra, this cutoff energy is difficult to determine with spectral fitting alone. We have used a new method that combines spatial, spectral, and temporal analysis to determine the cutoff energy for the M1.2 flare observed with *RHESSI* on 2002 April 15. A low-energy cutoff of 24 ± 2 keV is required to ensure that the assumed thermal emissions always dominate over nonthermal emissions at low energies (<20 keV) and that the spectral fitting results are consistent with the *RHESSI* light curves and images. With this cutoff energy, we obtain a total nonthermal energy in electrons of $(1.6 \pm 1) \times 10^{30}$ ergs that is comparable to the peak energy in the thermal plasma, estimated from *RHESSI* observations to be $(6 \pm 0.6) \times 10^{29}$ ergs assuming a filling factor of 1.

Subject headings: Sun: flares — Sun: X-rays, gamma rays

1. INTRODUCTION

One of the most remarkable aspects of solar flares is that such a large fraction of the released energy is transferred to kinetic energy of electrons and ions. Early observations have indicated that a considerable fraction of the flare energy (perhaps as much as 50%) is converted to accelerate electrons (Brown 1971; Lin & Hudson 1976) and ions (Ramaty et al. 1995). Clearly, verification and more accurate quantification of this result for a range of different flares is critical to an understanding of the mechanisms of particle acceleration and plasma heating.

The evaluation of the energy partition in flares between thermal plasma and nonthermal electrons is hampered by observational limits. Two of the main uncertainties in the measurements that compromise the evaluation of the energy budget are the filling factor of the thermal plasma and the low-energy cutoff in the nonthermal electron distribution. The filling factor ($f \leq 1$) is the ratio of the volume filled by hot X-ray–emitting plasma ($V_{\rm real}$) to the total source volume ($V_{\rm meas}$) estimated from the images. The thermal energy ($E_{\rm therm}$) is proportional to the square root of the filling factor as indicated in the following expression:

$$E_{\rm therm} = 3n_e V_{\rm real} kT = 3kT\sqrt{{\rm EM}V_{\rm real}} = 3kT\sqrt{{\rm EM}V_{\rm meas} f}, \quad (1)$$

where n_e is the plasma density, EM ($=n_e^2 V_{\rm real}$) and T are the emission measure and temperature of the thermal plasma, respectively, and k is the Boltzmann constant. It is often assumed that $f = 1$ but there are observations suggesting that it could be as low as 10^{-4} for coronal loops (e.g., Porter & Klimchuk 1995; Cargill & Klimchuk 1997). This immediately introduces a factor of 100 uncertainty in $E_{\rm therm}$ unless f can be more accurately estimated from observations.

Uncertainties in the low-energy cutoff of the nonthermal electron spectrum can lead to similar large uncertainties in the nonthermal energy. A low-energy cutoff is required to keep the total energy in electrons finite, given that electron spectra are steeper than E^{-2}, as determined from measured hard X-ray (HXR) spectra assuming thin- or thick-target interactions (Dennis 1985; Lin & Schwartz 1987; Winglee et al. 1991). Although a thermal bremsstrahlung model with multiple temperatures can usually fit the data (Brown 1974; Emslie & Brown 1980; Brown & Emslie 1987), power-law photon spectra above $\sim$10 keV are generally believed to be produced by bremsstrahlung emission from nonthermal electrons that themselves have a power-law energy distribution. Striking support for this nonthermal, thick-target bremsstrahlung interpretation comes from the observation of simultaneous (within a fraction of one second) impulsive HXR emissions from the two footpoints of a flare loop (e.g., Sakao 1994), as would be expected from the interaction of electron beams with the chromosphere.

Because of the high minimum photon energy detectable by most HXR spectrometers before *RHESSI* (typically $\geq$20 keV) and poor spectral resolution, and because of the presence of strong thermal bremsstrahlung at low energies, the low-energy cutoff in the electron distribution has been impossible to determine. Most previous estimations of the total electron energy have been made with assumed (arbitrary) cutoff energies in the range of 20–30 keV (Dennis et al. 2003, and references therein). Holman & Benka (1992) argued that the low-energy cutoff can, in fact, be determined from the spectral transition from thermal to nonthermal bremsstrahlung in their direct electric-field heating and acceleration model. Low-energy cutoffs ranging from 20 to 40 keV were obtained with this hybrid thermal/nonthermal model (Benka & Holman 1992). Gan (2001) and Gan et al. (2002) have found that many of the double-power law spectra obtained from the Burst and Transient Source Experiment (BATSE) on the *Compton Gamma Ray Observatory* (*CGRO*) are consistent with the flattening that results from a low-energy cutoff ranging from 45 to 97 keV. A low-energy cutoff as high as 73 keV has also been found late in the γ-ray line flare on 2003 July 23 (Holman et al. 2003).

The total energy of the nonthermal electrons is very sensitive to the low-energy cutoff, particularly for flares with steep

[1] Department of Physics, Catholic University of America, 620 Michigan Avenue NE, Washington, DC 20064; lhsui@stars.gsfc.nasa.gov.

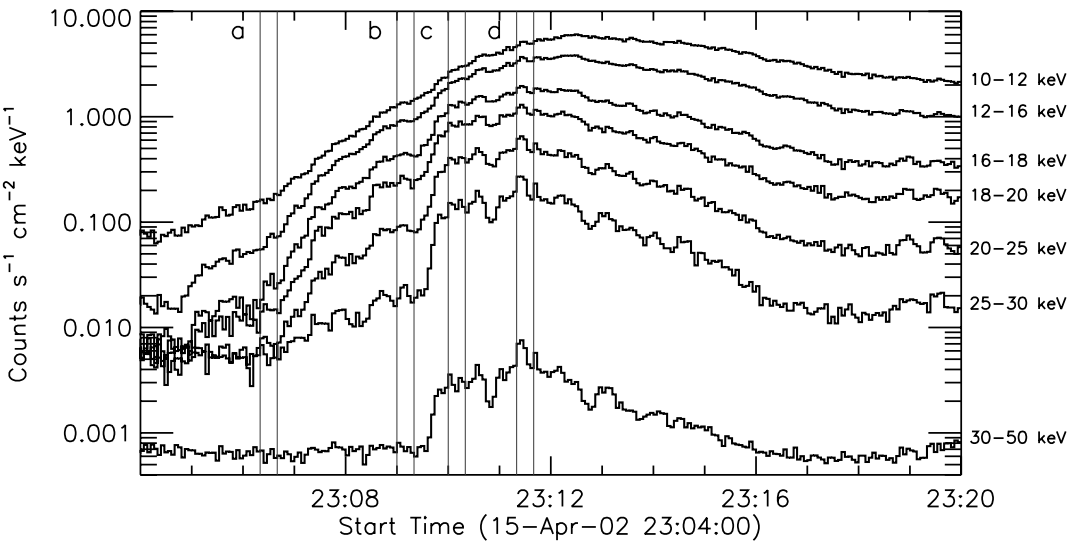

FIG. 1.—*RHESSI* light curves in seven energy bands for the flare on 2002 April 15. The time resolution is 4 s. The four time intervals indicated in the plot are for the four spectra in Fig. 4.

spectra. Dennis et al. (2003) reported the energetics of over 30 flares observed with the Hard X-Ray Imaging Spectrometer (HXIS) and the Hard X-Ray Burst Spectrometer (HXRBS) on the *Solar Maximum Mission* (*SMM*). For most of these flares there was considerably more energy in the electrons (above 25 keV, the HXRBS low-energy threshold) than in the thermal plasma. If a 10 keV cutoff was used instead, the total nonthermal energy would be an order of magnitude larger, on average. Saint-Hilaire & Benz (2002) obtained a similar result for a C9.7 flare observed with *RHESSI*. They found that the energy in nonthermal electrons above 10 keV was $(1.8–3.4)\times10^{30}$ ergs, while the thermal energy in what they called the flare kernel was only $(6–12)\times10^{28}$ ergs. However, they did find an additional $\sim10^{30}$ ergs in the ejecta. In the X4.8 γ-ray line flare observed with *RHESSI* on 2003 July 23, Holman et al. (2003) obtained upper limits on the low-energy cutoff that increased from $\sim$20 to $\sim$40 keV during the impulsive phase of the flare. In this way they obtained the minimum total energy in the nonthermal electrons that was of the same order as the energy in the thermal plasma. A similar result was reported for the X1.2 flare observed with *RHESSI* on 2002 April 21 (Emslie et al. 2004).

All the studies mentioned above have demonstrated that a power-law function can generally fit the measured HXR spectra. However, the low-energy cutoff is not uniquely determined. *RHESSI* spectra during the impulsive phase of a flare often show two components: a near exponential (thermal) component at low energies and a flatter power-law or double power-law (nonthermal) component at higher energies. The two components merge smoothly together. Electron spectra with a range of cutoff energies up to a maximum value produce photon spectra that are able to fit the same X-ray spectrum equally well. Any cutoff energy below that upper limit can still fit the data equally well because at low energies, the fluxes contributed from the nonthermal bremsstrahlung are usually much less than those from the thermal bremsstrahlung.

We report on a flare observed with *RHESSI* on 2002 April 15, one of the three homologous flares that occurred between 2002 April 14 and 16 (Sui et al. 2004). *RHESSI* observations of this flare are found to have distinctive characteristics that allow the low-energy cutoff to be more tightly constrained than has previously been possible. In the following sections, we explain how the low-energy cutoff is obtained, and how it affects the evaluation of the flare energetics. Earlier studies of this event by Sui & Holman (2003) and Sui et al. (2004) provided evidence for the existence of a large-scale current sheet above the flare loops. Multiwavelength analyses of this same event are also reported by L. Sui et al. (2005, in preparation).

2. DETERMINATION OF THE LOW-ENERGY CUTOFF

Although *RHESSI* covers energies down to $\sim$3 keV, we only considered spectral data above 10 keV for this paper. This is because the *RHESSI* thin attenuators were in throughout the flare observation. As a result, the effective area of the detectors drops rapidly at photon energies below 10 keV (Smith et al. 2002). The current uncertainty in the instrument response matrix is large at these energies. In addition, the counts below $\sim$5 keV are dominated by higher energy photons that suffer K escape when they are photoelectrically absorbed in the germanium detectors (Smith et al. 2002). Thus, no reliable information about the incident photon flux below this energy can be determined from the *RHESSI* observations with the attenuators in place.

The *RHESSI* light curves in seven energy bands for the flare are shown in Figure 1. The X-ray fluxes below 20 keV started to gradually increase at $\sim$23:05 UT. The fluxes above 20 keV did not increase until some two minutes later with the start of a small rise at 23:07:00 UT followed by an abrupt rise at 23:09:40 UT (characteristic of the start of the impulsive phase), and peaked at around 23:11:26 UT. Note that in both the rise and impulsive phases, the light curves at higher energies (>20 keV) are spikier than those at low energies. Since thermal emission results in a smooth flux time history, while nonthermal emission produces a spiky time history, the light curves seems to suggest that the thermal and nonthermal emissions dominate the fluxes below and above $\sim$20 keV, respectively.

RHESSI images in four energy bands at 23:08:40–23:09:40 UT (in the late rise phase) are shown in Figure 2. The images below 20 keV show a flare loop with a bright loop top. The reason the whole loop is not seen may be *RHESSI*'s limited image dynamic range of $\sim$20:1 based on current instrument calibrations (Hurford et al. 2002). The 20–30 keV image shows a loop top as well as a northern footpoint of the flare loop.

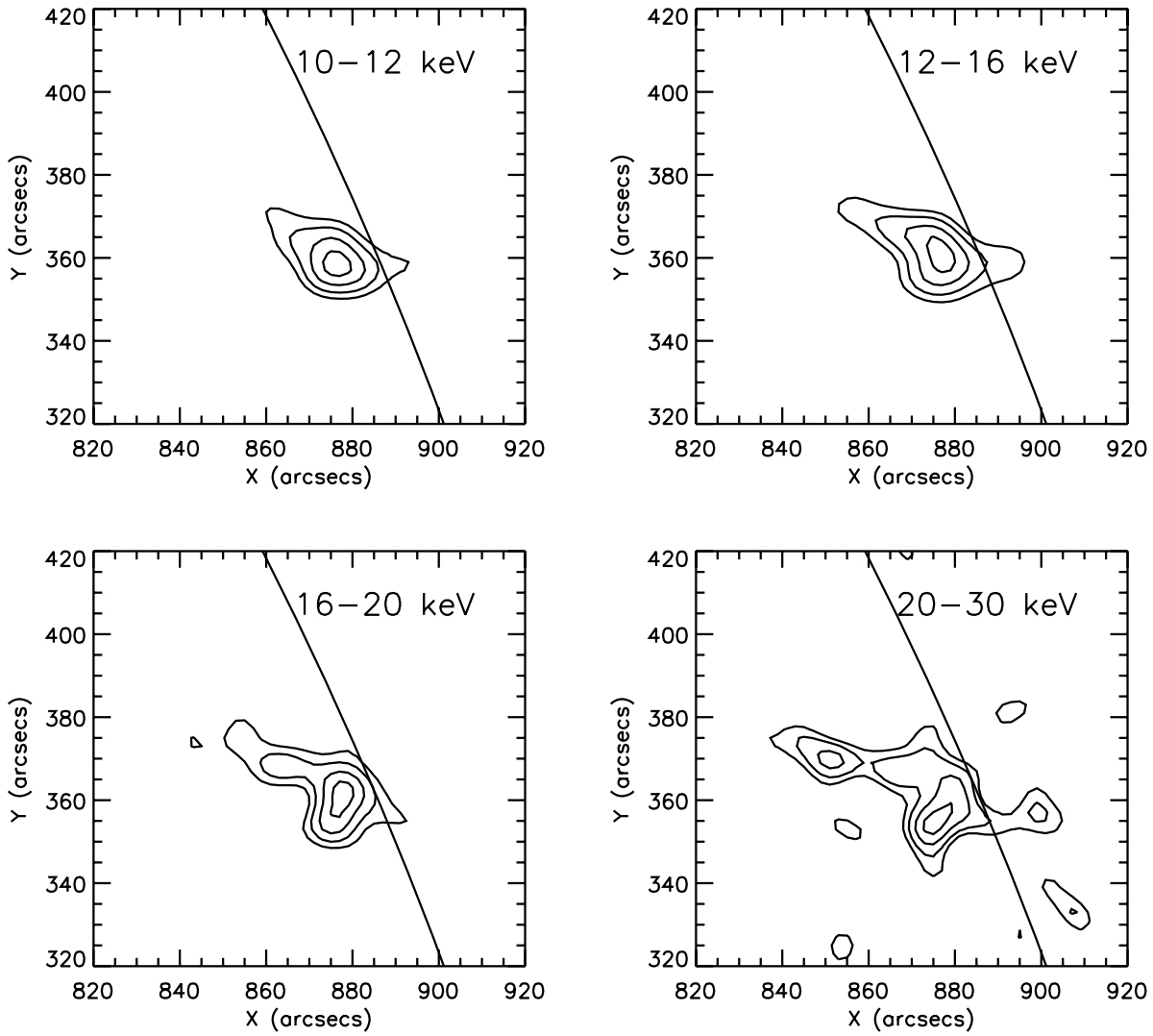

FIG. 2.—*RHESSI* images in four energy bands during the late rise phase (23:08:40–23:09:40 UT). The images are reconstructed with the CLEAN algorithm (Hurford et al. 2002) using grids 3–9, giving a spatial resolution of $\sim 7''$. The diagonal curve represents the solar limb.

Emission from footpoints is interpreted as thick-target bremsstrahlung from nonthermal electrons when they bombard the denser chromosphere. Therefore, the images suggest that thermal emission dominates at energies below 20 keV, while nonthermal emission contributes significantly at energies above 20 keV. This nonthermal interpretation is in agreement with the spiky flux variations above 20 keV seen in the light curves in the late rise phase (Fig. 1).

RHESSI images in different energy bands at the HXR peak (23:11–23:12 UT) are shown in Figure 3. At lower energies (<20 keV), the images still show a bright loop-top source. At higher energies (>20 keV), the images show two footpoints and an HXR loop-top source, with nonthermal emission from the southern footpoint dominating. The footpoints and the HXR loop-top source can be seen during most of the impulsive phase (from 23:09:40 to 23:13 UT). Unlike the previously reported HXR loop-top sources (Masuda et al. 1994, 1995; Petrosian et al. 2002; Sui et al. 2002), the HXR loop-top source of this flare is very bright, about a factor of 3 brighter than either footpoint in the 30–50 keV band except at the HXR peak when the southern footpoint was brightest. Veronig & Brown (2004) attributed this bright HXR loop-top source to thick-target bremsstrahlung from nonthermal electrons in the corona.

During the early rise phase (from 23:05 to 23:07 UT) when there is no evident increase in fluxes above 20 keV, the *RHESSI* spectra are well fitted with a model consisting solely of an isothermal bremsstrahlung spectrum in the energy range between 10 and 20 keV. Figure 4*a* shows one such spectrum at 23:06:20–23:06:40 UT. The temperature of the thermal plasma derived from the fit is 23 MK, and the emission measure is 4.0×10^{46} cm^{-3}.

The spectra during the late rise phase (from 23:07 to 23:09:40 UT) and the impulsive phase (after 23:09:40 UT) all have a power-law component at high energies. Because the photon fluxes above 20 keV are weak during the late rise phase, the power-law nonthermal components are not as distinct as those in the impulsive phase. However, the *RHESSI* images (the footpoint seen in 20–30 keV band in Fig. 2) and light curves (spiky flux variations above 20 keV in Fig. 1) during that period all indicate the authenticity of this nonthermal component. To fit these spectra, we used a model consisting of both a thermal bremsstrahlung component and a nonthermal thick-target bremsstrahlung component. The nonthermal electrons are assumed to have a single power-law distribution with a low-energy cutoff. One sample spectrum in the late rise phase (23:09:00–23:09:20 UT) and one in the impulsive phase (23:10:00–23:10:20 UT) are shown in Figures 4*b* and 4*c*. Because of its steep power law, if a very low

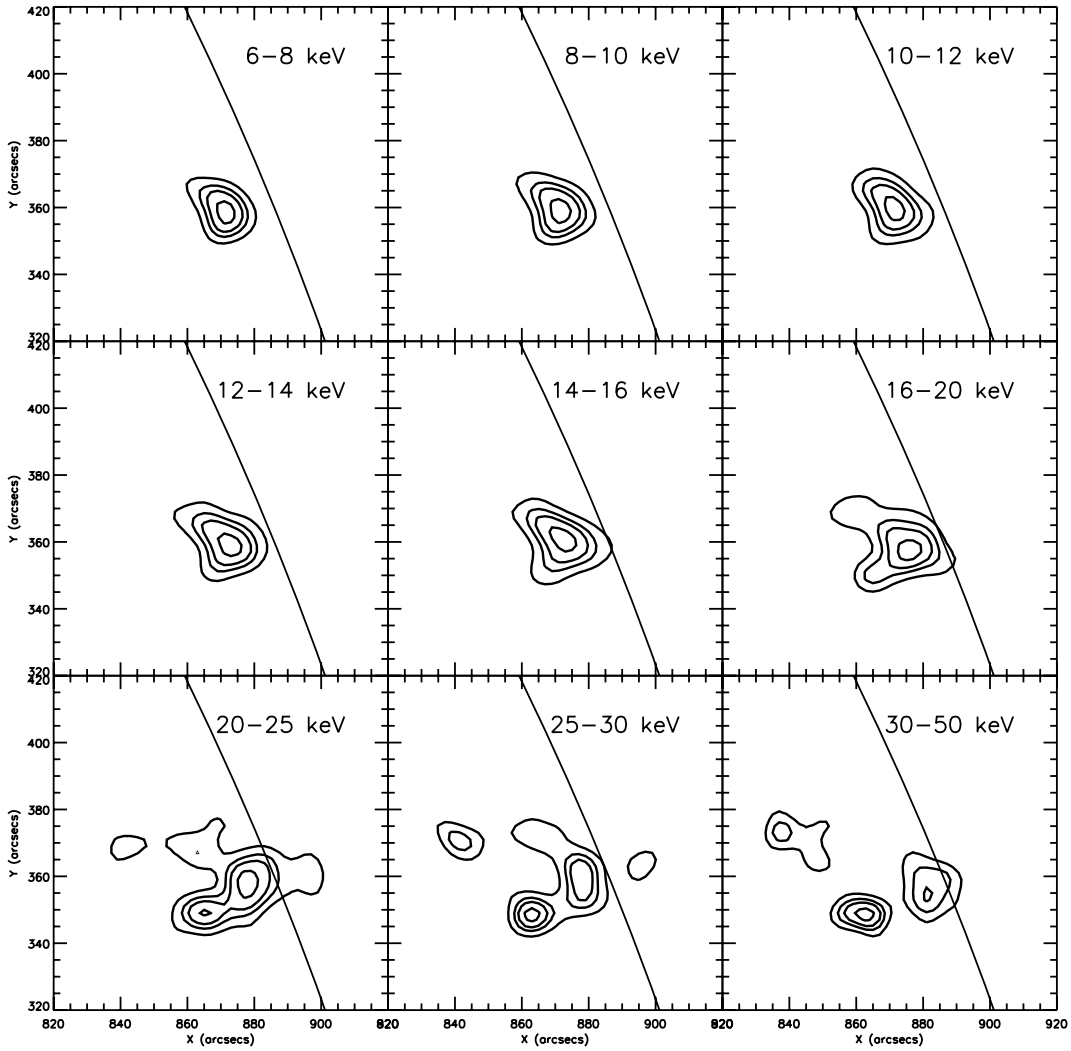

FIG. 3.—*RHESSI* images in nine energy bands at the HXR peak (23:11–23:12 UT). All other aspects are the same as in Fig. 2.

low-energy cutoff (say 10 keV) is allowed, the X-ray flux contributed from the nonthermal, power-law component at low energies would be as high as or higher than that from the thermal component. However, the *RHESSI* images shown in Figure 3 already suggest that the low-energy photon fluxes (<20 keV) are predominately thermal emission, since they come from the upper part of the flare loops. Moreover, the smoothly rising light curves (Fig. 1) are also consistent with a thermal interpretation at these low energies. Therefore, there must be a lower limit to the low-energy cutoff to ensure that the predicted fluxes of nonthermal bremsstrahlung at the low energies are well below those of the thermal bremsstrahlung.

To determine the low-energy cutoff, instead of letting it be a free parameter, we set the cutoff energy to different fixed values when fitting the spectra throughout the flare. We do not mean that the cutoff energy should be constant throughout the flare. Instead, we try to provide an acceptable range for the low-energy cutoff. Because most of the spectra do not have an apparent exponential (thermal) component at low energies (Fig. 4*c*), if we allow the low-energy cutoff to be a free parameter, it would be impossible to fit the spectra consistently. The variation of the obtained cutoff energies would be so large that the temperature and emission measure would not have smooth time histories. Moreover, a cutoff energy that varies significantly with time cannot ensure that the thermal flux dominates at low energies.

Any determination of the low-energy cutoff has to ensure that the following three conditions are satisfied:

1. The spectral fitting to the measured X-ray spectrum must give satisfactory values for the reduced chi-squared ($\chi_r^2 \approx 1$).
2. When the impulsive phase starts, the thermal parameters, i.e., the temperature and emission measure, should not suddenly decrease. In other words, the time profiles of the thermal parameters should have a smooth and gradual evolution over the transition from the rise to the impulsive phase of the flare.
3. Thermal emission must dominate at photon energies below ~20 keV, and nonthermal emission must dominate at energies above ~20 keV, so as to be consistent with the *RHESSI* images and light curves.

Figure 5 shows the time profiles of T and EM of the thermal plasma obtained from spectral fitting with different low-energy cutoffs. The thick solid lines indicate results for a 24 keV low-energy cutoff. The dotted lines and thin solid lines are for low-energy cutoffs lower and higher than 24 keV, respectively. In the early rise phase (before 23:07 UT), no nonthermal component was needed, and hence only an isothermal bremsstrahlung model was used with the best-fit T and EM as shown. Starting at 23:07:00 UT, a nonthermal thick-target bremsstrahlung model was added to the isothermal bremsstrahlung function in order to fit the spectra.

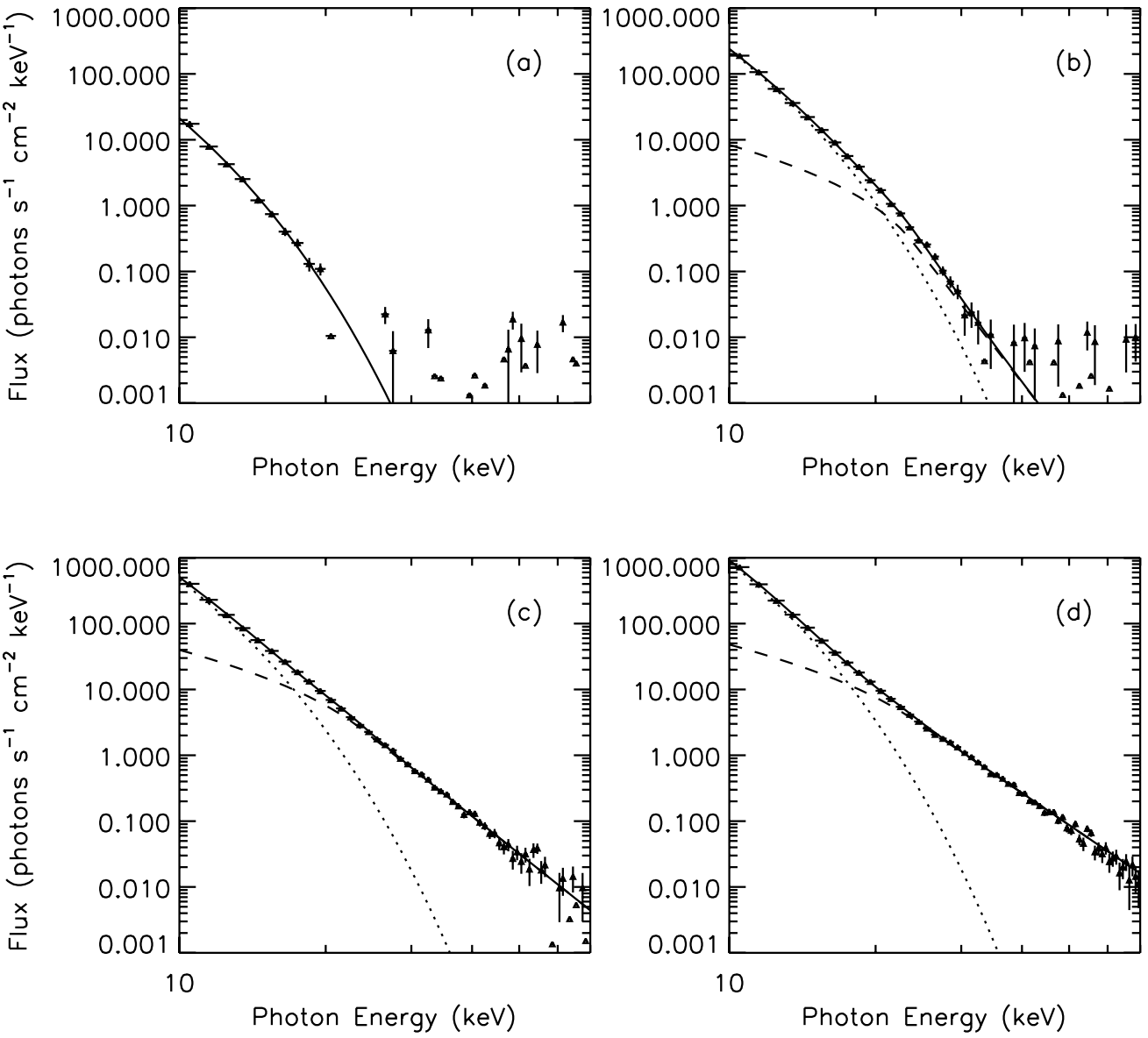

FIG. 4.—*RHESSI* spatially integrated spectra in four time intervals. The time intervals are indicated graphically in Fig. 1. (*a*) Spectrum at 23:06:20–23:06:40 UT (early rise phase). (*b*) Spectrum at 23:09:00–23:09:20 UT (just before impulsive phase). (*c*) Spectrum at 23:10:00–23:10:20 UT (soon after the impulsive rise). (*d*) Spectrum at 23:11:00–23:11:20 UT (at the HXR peak). The plus signs with error bars represent the spectral data. The lines represent model spectral fits: the dashed lines are for nonthermal thick-target bremsstrahlung, the dotted lines are for thermal bremsstrahlung, and the solid lines are for the summation of the two.

The following considerations were taken into account in evaluating the spectral fitting results:

1. Fits with low-energy cutoffs $\leq$28 keV give equally good values of χ_r^2 ($\sim$1.0). The value of χ_r^2 increases when the value of the low-energy cutoff increases, indicating that the fits get worse for low-energy cutoffs above $\sim$30 keV. For instance, spectral fitting with a 36 keV low-energy cutoff gives $\chi_r^2 \approx 2.3$, double that obtained with a low-energy cutoff of $\leq$28 keV. In the *RHESSI* Object Spectral Executive (OSPEX), ± 1 σ statistical uncertainties and 5% systematic uncertainties were used in the calculation of χ_r^2. Since the correct systematic uncertainties are unknown for *RHESSI*, the value of χ_r^2 can only be used for relative comparison purposes.

2. From Figure 5, we find that a low-energy cutoff at 24 $\pm$ 2 keV gives a smooth time profile for both emission measure and temperature over the transition from the rise to the impulsive phase of the flare. The low-energy cutoff of 20 keV causes a sudden decrease in emission measure at the start of the impulsive phase. Moreover, the plasma temperature obtained with this 20 keV cutoff energy starts to decrease after 23:07 UT, when nonthermal emission starts indicating an increase in the energy release rate. This is improbable, since substantially increased plasma heating should have occurred at this time. On the other hand, low-energy cutoffs above 26 keV cause a sudden increase in temperature at the impulsive rise. This may be possible, considering the increased plasma heating by the stronger nonthermal electron beam, i.e., the Neupert effect (Neupert 1968; Dennis & Zarro 1993), or by another direct heating process, e.g., slow-mode shock (Cargill & Priest 1982) or direct Joule heating (Holman 1985). However, these values of the low-energy cutoff also cause a sudden decrease in emission measure, which is not likely. Simultaneous increases in both temperature and emission measure during the impulsive phases of flares have been seen before (e.g., Holman

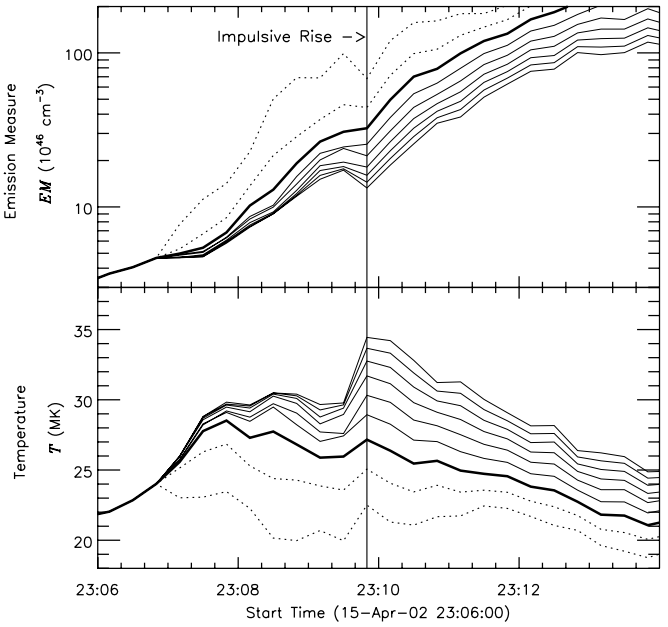

FIG. 5.—Time profiles of emission measure (*top*) and temperature (*bottom*) of the thermal plasma obtained from *RHESSI* spectral fitting with different electron low-energy cutoffs. During the early rise phase of the flare (before 23:07:00 UT) only an isothermal bremsstrahlung model is used, so no low-energy cutoff is needed. A thick-target bremsstrahlung component with different electron low-energy cutoffs is added to fit the spectra at later time intervals. In the top panel, the lines show the plasma emission measures obtained with electron low-energy cutoffs of (*from top to bottom*) 20, 22, 24, . . . , 34, 36 keV, in steps of 2 keV. In the bottom panel, the lines show the plasma temperatures obtained with electron low-energy cutoffs (*from top to bottom*) 36, 34, . . . , 24, 22, 20 keV, in steps of 2 keV. In both panels, the low-energy cutoff for the thick solid lines is 24 keV.

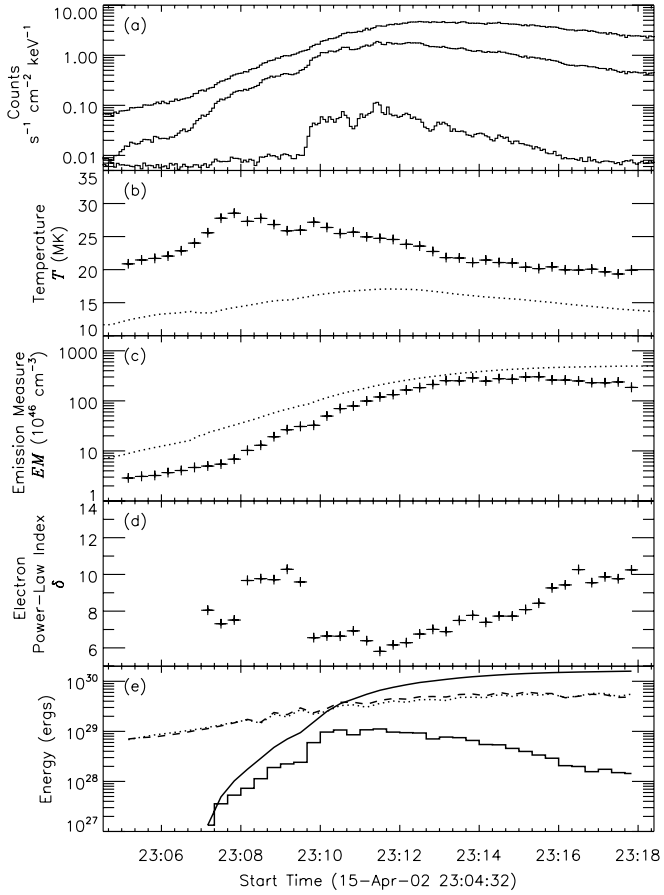

FIG. 6.—*RHESSI* spectral fit results with a 24 keV low-energy cutoff in the electron flux distribution. (*a*) *RHESSI* light curves in energy bands (*from top to bottom*): 6–12, 12–25, and 25–50 keV. (*b*) Plasma temperatures from *RHESSI* (*plus signs*) and *GOES* (*dotted line*). (*c*) Plasma emission measures from *RHESSI* (*plus signs*) and *GOES* (*dotted line*). (*d*) Electron flux distribution power-law indices obtained with the thick-target bremsstrahlung model. (*e*) Thermal plasma energy from *RHESSI* (*dashed line*) and *GOES* (*dotted line*, barely distinguishable from the dashed line). The solid line represents the accumulated nonthermal electron energy. The histogram represents the nonthermal electron energy deposited into a thick target in each 20 s time interval.

et al. 2003). We believe that this sudden increase in temperature accompanied by a sudden decrease in emission measure is solely caused by spectral fitting with an incorrect low-energy cutoff.

3. With the 24 ± 2 keV low-energy cutoff, the thermal and nonthermal components, as indicated in the spectra shown in Figures 4*b* and 4*c*, are about equal at ~20 keV with the thermal emission dominating at lower energies and nonthermal at higher energies. This is, in general, consistent with the *RHESSI* light curves and images. Moreover, with this 24 keV cutoff energy, we find the nonthermal component contributes to the total emission in energy bands as low as 12 keV. For instance, in the spectrum at 23:10:00–23:10:20 UT (Fig. 4*c*), the nonthermal component contributes ~15% of the total flux at 12 keV. This can explain the small bumpy components appearing on top of the smooth light curves in the three energy bands between 12 and 20 keV seen in Figure 1. The *RHESSI* spectrum at the HXR peak (23:11:20–23:11:40 UT), fitted with the 24 keV low-energy cutoff, is shown in Figure 4*d*. Because the power-law nonthermal spectrum is flattest at the HXR peak, a thermal component is clearly evident above an extrapolation of the power-law nonthermal component at energies greater than 20 keV to low energies.

The time profiles of the spectral fit parameters with the 24 keV low-energy cutoff are plotted in Figures 6*b*–6*d*. For comparison purposes, the *GOES* temperature and emission measure, obtained with the code recently developed by White et al. (2005) using the more up-to-date Chianti atomic model (ver. 4.2; see Young et al. 2003), are also plotted. The temperatures obtained from *GOES* are lower than those from *RHESSI*, while the emission measures are always higher, showing that the plasma must be multithermal. This is consistent with the fact that *RHESSI* is more sensitive to the high-temperature plasma, while *GOES* is more sensitive to somewhat lower temperature plasma. White et al. (2005) found that the Mewe atomic model (Mewe et al. 1985), used for the current *GOES* Workbench in Solar Software, gives temperatures of ~1–2 MK lower and emission measures up to a factor of 4 larger than results obtained with the Chianti model. The time profile of the electron flux distribution power-law index shown in Figure 6*d* indicates a "soft-hard-soft" pattern (e.g., Dennis 1985; Grigis & Benz 2004). There is a sudden hardening (power index decreasing from 9.6 to 6.6) at 23:09:40 UT, different from the typical, more gradual "soft-hard-soft" pattern. This is due to the sudden increase in the HXR fluxes above 30 keV at that time. The early spectra from 23:07 to 23:08 UT are harder than the following spectra and, therefore, do not fit the "soft-hard-soft" pattern. However, because the photon flux above 20 keV is low in this period, the uncertainty in the obtained power-law indices is large.

3. THERMAL AND NONTHERMAL ENERGIES

To calculate the total energy in accelerated electrons, we first obtain the nonthermal energy input in each time interval (Fig. 6*e*,

histogram) by integrating the power-law electron spectrum above the cutoff energy of 24 keV. The resulting nonthermal energies are then accumulated in time (Fig. 6*e*, *solid curve*) to give a total of $(1.6 \pm 1) \times 10^{29}$ ergs. The uncertainty estimation is based on the 2 keV uncertainty in the 24–keV low-energy cutoff in the electron spectrum. Since this low-energy cutoff energy was not arbitrarily selected but determined from the *RHESSI* observations, we believe that the nonthermal energy obtained here is more reliable than any previously obtained.

The thermal energy (Fig. 6*e*, dotted line for *GOES*, dashed line for *RHESSI*) is calculated using equation (1). The filling factor was set to 1, giving an upper limit to the thermal energy. The temperature and emission measure from *GOES* and *RHESSI* are given in Figures 6*b* and 6*c*. The source volume at each time interval is estimated from the source area in the *RHESSI* images in a manner similar to that used by Emslie et al. (2004), i.e., $V_{\rm meas} = A^{3/2}$, where A is the source area inside the 50% contour of the 10–20 keV image at each time interval. The images were obtained using the CLEAN algorithm (Hurford et al. 2002) with detectors 3–9. The estimated source volume is $(1-2) \times 10^{27}$ cm^3. Because of the low count rate in the early rise phase, the image quality from 23:05 to 23:07:40 UT is not good enough for this area estimation method. Consequently, we set the area before 23:08 UT to be the same as the area obtained from the image at 23:08 UT. The source volumes for the *GOES* analysis were assumed to be the same as those obtained from *RHESSI*.

As shown in Figure 6*e*, the thermal energies obtained with *GOES* and *RHESSI* are almost equal throughout the flare, indicating that the energy contents of the plasma with different temperature are the same. For comparison purposes, we also used the current *GOES* Workbench (based on the Mewe atomic model) to derive the *GOES* plasma temperature and emission measure. The resulting *GOES* thermal energy was found to be larger than the thermal energy obtained with *RHESSI* by a factor of 2 throughout the flare.

The thermal energy of the flare is taken to be the peak value of the energy content of the thermal plasma. It is $\sim 5.7 \times 10^{29}$ ergs derived from *GOES* and $(6.0 \pm 0.6) \times 10^{29}$ ergs from *RHESSI*, both using a volume of $\sim 1.8 \times 10^{27}$ cm^3. The error estimation for the thermal energy from *RHESSI* is based only on the uncertainties in T and EM caused by the ± 2 keV uncertainty in the electron low-energy cutoff. Because we do not account for thermal energy loss due to plasma cooling and any heating at later times, the obtained thermal energy is a lower limit. On the other hand, if the filling factor of the thermal plasma is less than 1, the thermal energy is overestimated. Taking these uncertainties into account, it is fair to conclude that the total nonthermal energy is comparable to the thermal energies estimated using *GOES* and *RHESSI*, agreeing with the earlier results (e.g., Saint-Hilaire & Benz 2002; Dennis et al. 2003; Holman et al. 2003; Emslie et al. 2004).

4. SUMMARY AND DISCUSSION

The low-energy cutoff of the electron distribution has generally been decided in the past by the lower energy limit of the spectrometer being used or set to some arbitrary value. This leads to large uncertainties in estimating the total nonthermal energies in flares. The specific characteristics of this flare on 2002 April 15 allowed us to determine a low-energy cutoff to the nonthermal electron spectrum with greater certainty than has previously been possible. To ensure the dominance of the thermal flux at low energies and a smooth evolution of the thermal parameters over the transition from the rise to the impulsive phase of the flare, we found the low-energy cutoff of the nonthermal electrons must be 24 ± 2 keV. As a result, the total energy in the nonthermal electrons is calculated to be $(1.6 \pm 1.0) \times 10^{30}$ ergs, compared to the total thermal energy in hot plasma of $\sim 5.7 \times 10^{29}$ ergs from *GOES* and $(6 \pm 0.6) \times 10^{29}$ ergs from *RHESSI*.

It is interesting to notice that the 24 ± 2 keV cutoff energy obtained here agrees with the recent result reported by Veronig et al. (2005) for this flare using the Neupert effect. Assuming that thick-target Coulomb collisions of nonthermal electrons with ambient plasma is the source of heating and mass supply in the flare, Veronig et al. found that in order to account for the energy deposited into the hot plasma (conductive and radiative energy losses were included), the low-energy cutoff to the nonthermal electron distributions should be in the range of about 23–26 keV.

This event is somewhat special because of its steep HXR spectrum—the electron power-law index was -6 or steeper. Thus, if the low-energy cutoff for the nonthermal electrons were very low, the fluxes of the nonthermal power-law component would be as high as or higher than the thermal component at lower energies. This is contradictory to the fact that thermal emission appears to dominate in *RHESSI* images and light curves at energies below $\sim$20 keV. For many flares, the power-law component will not dominate at lower energies, even for a low-energy cutoff as low as 1 keV. Therefore, the method we used to estimate the low-energy cutoff for this event will not be applicable for all events.

The following analysis techniques can be recommended for future work based on the results presented here. Instead of fitting only one or a few spectra, we should fit spectra throughout the flare to find the most reasonable model(s). In fact, some of the spectra during the impulsive phase of the 2002 April 15 flare can be fitted with just a single power-law function all the way down to 7 keV. However, this kind of fitting scenario is contradictory to the spectral fits in the rise phase, which indicate that the spectra at lower energies are thermal. Sui et al. (2002) have pointed out that multiple models could be used to fit the same *RHESSI* spectrum. Certainly, fitting multiple spectra throughout the flare allows a check for a consistent time history for temperature and emission measure. In the future, we can also try to utilize other sources of information, such as checking the effect of a low-energy electron cutoff on microwave spectra (Holman 2003) and checking plasma temperatures independently determined from the two iron-line complexes at $\sim$6.7 and $\sim$8 keV in *RHESSI* spectra (Phillips 2004). All these techniques are under study.

The spectral fitting results should be checked against *RHESSI* images for consistency. We can check whether or not the energy ranges in the fitted spectra that are dominated by thermal or nonthermal emission also show evidence for thermal or nonthermal emission, respectively in the *RHESSI* images. Usually the X-ray loop sources are due to thermal bremsstrahlung emission, and footpoints are due to nonthermal thick-target bremsstrahlung. However, we have to be careful in judging which sources are thermal or nonthermal in the *RHESSI* images. For instance, Holman et al. (2003) found that an extended coronal source in the rise phase of the 2002 July 23 X4.8 flare could not be fitted by an isothermal bremsstrahlung model. Instead, it could be fitted with a broken power-law model, leading to a nonthermal thick-target interpretation (Lin et al. 2003). Veronig & Brown (2004) found that the HXR coronal sources (>25 keV) in the 2002 April 14–15 and April 15 flares analyzed by Sui et al. (2004) can be interpreted as nonthermal thick-target emission, which agrees with our interpretation in this paper. Our preliminary spectral analysis

of the other two homologous flares on 2002 April 14–15 and 16 indicates that they have the same characteristics as this event. Therefore, the techniques developed here will be applied to other events in future studies.

One interesting finding, as indicated in Figure 6*b*, is that the plasma temperature obtained with *RHESSI* peaked *before* the impulsive rise of the HXR flux. When the impulsive phase started, no significant change in the rate of increase of the thermal energy is apparent at this time. This suggests that direct plasma heating is more significant than the heating by the nonthermal electrons in this flare. The lower temperature plasma observed with *GOES*, however, reaches its highest temperature after the impulsive peak of the flare. This interesting behavior will be studied in a future paper.

We acknowledge the whole *RHESSI* team, without which none of this work would be possible. We thank Stephen White and Astrid Veronig for providing the code to calculate *GOES* temperatures and emission measures. We also thank the referee, Astrid Veronig, for insightful comments that resulted in significant improvements to the paper.

REFERENCES

Benka, S. G., & Holman, G. D. 1992, ApJ, 391, 854
Brown, J. C. 1971, Sol. Phys., 18, 489
———. 1974, in IAU Symp. 57, Coronal Disturbances, ed. G. A. Newkirk, Jr. (Dordrecht: Reidel), 395
Brown, J. C., & Emslie, A. G. 1987, Sol. Phys., 110, 305
Cargill, P. J., & Klimchuk, J. A. 1997, ApJ, 478, 799
Cargill, P. J., & Priest, E. R. 1982, Sol. Phys., 76, 357
Dennis, B. R. 1985, Sol. Phys., 100, 465
Dennis, B. R., Veronig, A., Schwartz, R. A., Sui, L., Tolbert, A. K., & Zarro, D. M. 2003, Adv. Space Res., 32(12), 2459
Dennis, B. R., & Zarro, D. M. 1993, Sol. Phys., 146, 177
Emslie, A. G., & Brown, J. C. 1980, ApJ, 237, 1015
Emslie, A. G., et al. 2004, J. Geophys. Res., 109, 10104
Gan W. 2001, ApJ, 552, 858
Gan, W. Q., Li, Y. P., Chang, J., & McTiernan, J. M. 2002, Sol. Phys., 207, 137
Grigis, P. C., & Benz, A. O. 2004, A&A, 426, 1093
Holman, G. D. 1985, ApJ, 293, 584
———. 2003, ApJ, 586, 606
Holman, G. D., & Benka, S. G. 1992, ApJ, 400, L79
Holman, G. D., Sui, L., Schwartz, R. A., & Emslie, A. G. 2003, ApJ, 595, L97
Hurford, G. J., et al. 2002, Sol. Phys., 210, 61
Lin, R. P., & Hudson, H. S. 1976, Sol. Phys., 50, 153
Lin, R. P., Krucker, S., Holman, G. D., Sui, L., Hurford, G. J., & Schwartz, R. A. 2003, in Proc. 28th International Cosmic Ray Conference, ed. T. Kajita et al. (Tokyo: Univ. Academy Press), 3207
Lin, R. P., & Schwartz, R. A. 1987, ApJ, 312, 462
Masuda, S., Kosugi, T., Hara, H., Sakao, T., Shibata, K., & Tsuneta, S. 1995, PASJ, 47, 677
Masuda, S., Kosugi, T., Hara, H., Tsuneta, S., & Ogawara, Y. 1994, Nature, 371, 495
Mewe, R., Gronenschild, E. H. B. M., & van den Oord, G. H. J. 1985, A&AS, 62, 197
Neupert, W. M. 1968, ApJ, 153, L59
Petrosian, V., Donaghy, T. Q., & McTiernan, J. M. 2002, ApJ, 569, 459
Phillips, K. J. H. 2004, ApJ, 605, 921
Porter, L. J., & Klimchuk, J. A. 1995, ApJ, 454, 499
Ramaty, R., Mandzhavidze, N., Kozlovsky, B., & Murphy, R. J. 1995, ApJ, 455, L193
Saint-Hilaire, P., & Benz, A. O. 2002, Sol. Phys., 210, 287
Sakao, T. 1994, Ph.D. thesis, Univ. Tokyo
Smith, D. M., et al. 2002, Sol. Phys., 210, 33
Sui, L., & Holman, G. D. 2003, ApJ, 596, L251
Sui, L., Holman, G. D., & Dennis, B. R. 2004, ApJ, 612, 546
Sui, L., Holman, G. D., Dennis, B. R., Krucker, S., Schwartz, R. A., & Tolbert, K. 2002, Sol. Phys., 210, 245
Veronig, A. M., & Brown, J. C. 2004, ApJ, 603, L117
Veronig, A. M., Brown, J. C., Dennis, B. R., Schwartz, R. A., Sui, L., & Tolbert, A. M. 2005, ApJ, 621, 482
White, S. M., Thomas, R. J., & Schwartz, R. A. 2005, Solar Phys., in press
Winglee, R. M., et al. 1991, ApJ, 375, 366
Young, P. R., Del Zanna, G., Landi, E., Dere, K. P., Mason, H. E., & Landini, M. 2003, ApJS, 144, 135